

2004

Electromechanical actuation of composite material from carbon nanotubes and ionomeric polymer

Igor A. Levitsky

University of Rhode Island, igor_levitsky@uri.edu

P. Kanelos

University of Rhode Island

William B. Euler

University of Rhode Island, billeuler@uri.edu

Follow this and additional works at: https://digitalcommons.uri.edu/chm_facpubs

Citation/Publisher Attribution

Levitsky, I. A., Kanelos, P., & Euler, W. B. (2004). Electromechanical actuation of composite material from carbon nanotubes and ionomeric polymer. *The Journal of Chemical Physics*, 121(2), 1058-1065. doi: 10.1063/1.1760734

Available at: <http://dx.doi.org/10.1063/1.1760734>

This Article is brought to you by the University of Rhode Island. It has been accepted for inclusion in Chemistry Faculty Publications by an authorized administrator of DigitalCommons@URI. For more information, please contact digitalcommons-group@uri.edu. For permission to reuse copyrighted content, contact the author directly.

Electromechanical actuation of composite material from carbon nanotubes and ionomeric polymer

Terms of Use

All rights reserved under copyright.

Electromechanical actuation of composite material from carbon nanotubes and ionomeric polymer

I. A. Levitsky, P. Kanelos, and William B. Euler

Citation: *The Journal of Chemical Physics* **121**, 1058 (2004); doi: 10.1063/1.1760734

View online: <https://doi.org/10.1063/1.1760734>

View Table of Contents: <http://aip.scitation.org/toc/jcp/121/2>

Published by the [American Institute of Physics](#)

Articles you may be interested in

[Micromechanics of actuation of ionic polymer-metal composites](#)

Journal of Applied Physics **92**, 2899 (2002); 10.1063/1.1495888

[Comparative experimental study of ionic polymer–metal composites with different backbone ionomers and in various cation forms](#)

Journal of Applied Physics **93**, 5255 (2003); 10.1063/1.1563300

[An explicit physics-based model of ionic polymer-metal composite actuators](#)

Journal of Applied Physics **110**, 084904 (2011); 10.1063/1.3650903

[Charge dynamics in ionic polymer metal composites](#)

Journal of Applied Physics **104**, 104915 (2008); 10.1063/1.3017467

[On the capacitance-boost of ionic polymer metal composites due to electroless plating: Theory and experiments](#)

Journal of Applied Physics **105**, 104911 (2009); 10.1063/1.3129503

[Electromechanical response of ionic polymer-metal composites](#)

Journal of Applied Physics **87**, 3321 (2000); 10.1063/1.372343

PHYSICS TODAY

WHITEPAPERS

ADVANCED LIGHT CURE ADHESIVES

Take a closer look at what these environmentally friendly adhesive systems can do

READ NOW

PRESENTED BY
 **MASTERBOND**
ADHESIVES | SEALANTS | COATINGS

Electromechanical actuation of composite material from carbon nanotubes and ionomeric polymer

I. A. Levitsky

Emitech Inc., Fall River, Massachusetts 02720

P. Kanelos and William B. Euler

Department of Chemistry, University of Rhode Island, Kingston, Rhode Island 02881

(Received 22 January 2004; accepted 21 April 2004)

An actuating system composed of nafion ionomeric polymer coated with single-walled carbon nanotubes electrodes was studied as an electromechanical actuator. The actuator gives a sizable mechanical response to low voltages (turn-on voltage of ~ 2.5 V) under open-air conditions, i.e., in the absence of a surrounding supporting electrolyte. The actuator is active under both dc and ac bias and has a strong resonance at low frequencies which is dependent upon the size of the actuator. The actuator was studied using Fourier transform infrared and vis-NIR spectroscopies, cyclic voltammetry, and by the current-time response under an applied step voltage. An analytical model is proposed to understand the electrical behavior, which is consistent with the spectroscopic results.

© 2004 American Institute of Physics. [DOI: 10.1063/1.1760734]

I. INTRODUCTION

There is an increasing interest in using electroactive polymers that convert electrical energy into mechanical energy for numerous applications in MEMS/NEMS technology.¹ Electrochemical and electromechanical properties of ionomeric polymer-metal composites² (IPMCs) have attracted great attention due to their ability to provide effective mechanical actuation under low bias (several volts), high strain with respect to ferroelectric polymers, such as PVDF,³ and relatively fast response time compared to ionic gels⁴ and conductive polymers.⁵ The most studied IPMC material is nafion (a perfluorinated ionomer), a membrane with electrochemically plated Pt electrodes on both sides. The actuation mechanism of this composite was described in terms of electro-osmotic water transport driven by solvated cations and charging of the double layer at the interface between nafion and platinum^{2b} or an interfacial stress (nafion/Pt) inducing the composite motion.⁶ Recently, a general model was proposed taking into account both the hydraulic and the electrostatic effects in the IPMC.^{7,8}

The discovery of single-walled carbon nanotube (SWNT) electromechanical actuation⁹ introduced a unique material enabling the conversion of an electrical stimulus to mechanical displacement due to a novel quantum mechanical mechanism. For low charge density, SWNT mats demonstrate expansion and contraction with electron injection and hole injection, respectively.^{9(a),9(b)} However, at high charge density the electrostatic effect dominates and material expansion occurs regardless of the charge sign (Ref. 9(a) and references therein). Therefore, such an actuating system, at high charge density, principally cannot work in the bimorph cantilever geometry when asymmetrical electromechanical properties of both sides are required for cantilever bending. Also, SWNT actuation needs an electrolytic solution to provide a high charge concentration in the SWNT/electrolyte interface (double layer). Since ionomeric polymers represent a solid electrolyte, their coupling with SWNTs, as electrodes, could

result in an efficient novel actuating system utilizing the advantages of IPCM and SWNT materials. Recently, actuation of a SWNT-nafion composite prepared by the polymer doping of purified carbon nanotubes was reported.¹⁰ A high SWNT conductivity through a percolation pathway within the composite resulted in the displacement of the cantilever with platinum electrodes (Pt concentration was maintained below the doping metal level causing an independent nafion actuation).¹⁰ The carbon nanotubes in the study serve only as a highly conductive filler in the polymer matrix and therefore cannot exhibit their own actuation.

In this paper we report the electrochemical and electromechanical properties of a composite material prepared by spraying SWNTs onto both sides of a nafion membrane. Such a composite structure allows not only the investigation of electrochemical processes at the nafion-SWNT interface but also amplifies the actuation with respect to pure SWNT mats or IPMCs. Indeed, the SWNT cathode should exhibit its own stretching at low bias voltage (quantum effect) which coincides with the nafion stretching due to hydraulic and electrostatic effects. In addition, as we will demonstrate, this composite exhibits an efficient actuation in the open air as distinct from SWNT mats and most IPMCs, which require a liquid environment.

II. EXPERIMENT

SWNTs were synthesized by the arc discharge method and purified (85%) using air oxidation, acid treatment, and thermal annealing, as purchased from BuckyUSA, Inc. The average diameter of the nanotubes was in the range of 0.8–1.1 nm according to NIR absorption/Raman spectroscopy and TEM observation. Nafion 117 membrane (180 μm thickness, H^+ -exchanged form) was purchased from Aldrich. The SWNT/nafion/SWNT composite was prepared by airbrush spraying of a SWNT suspension in chloroform (~ 0.8 mg/ml, 30 min sonication) onto both sides of nafion at 50–60 °C. The deposited SWNTs form uniform and dense films (thick-

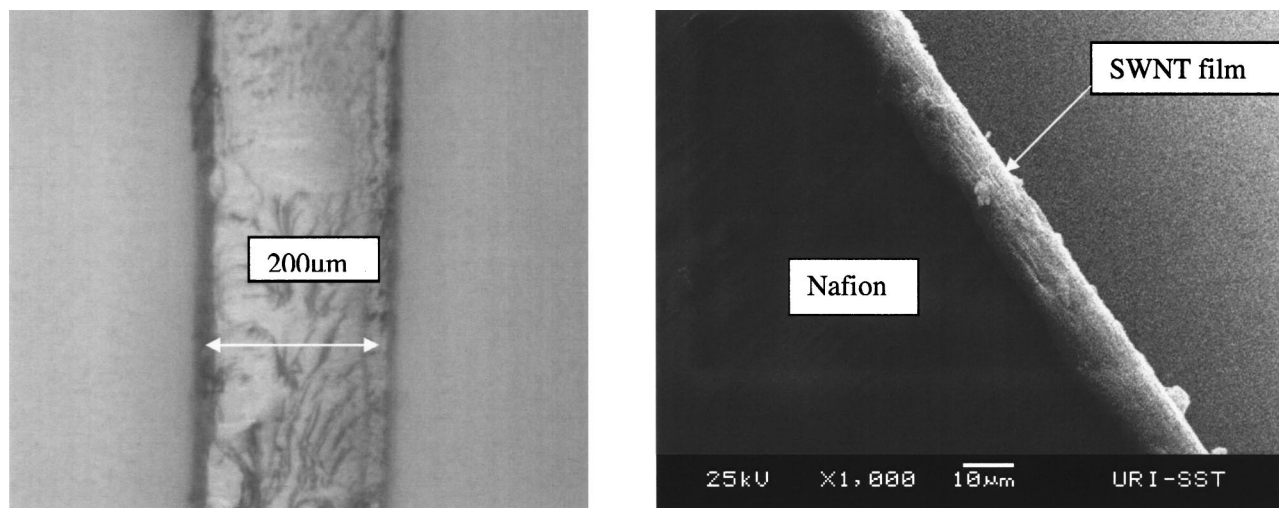


FIG. 1. Optical (left) and SEM (right) images of the cross section of SWNT/nafion/SWNT composite. SWNT film thickness is about 15 μm .

ness about 15–20 μm) with a high adhesion to the polymer surface (Fig. 1). Neither spin-cast nor coating methods could provide the same film quality. The reference samples graphite/nafion/graphite and gold/nafion/gold were prepared by the airbrush technique at the same conditions and gold sputtering (100 nm thickness), respectively. Additional sets of reference samples, for testing of possible actuation of SWNTs without nafion in the open air, were prepared by nanotube spraying onto the following substrates: glass, paper, polyethylene (a nonionomeric polymer), and nanoporous alumina oxide soaked in the NaCl (1M) solution. Finally, a bimorph cantilever was fabricated from the composite to form a strip ($\sim 3 \times 20 \text{ mm}^2$) and was clamped between two glass slides using platinum foil to maximize electrical contact with the voltage source.

I - V characteristics and current time scans in response no step voltage were carried out with a Keithley-236 source-measure unit. Cantilever displacement was measured by a video camera coupled with an optical microscope and connected to a computer video capture card. A Perkin-Elmer Lambda 900 was employed to detect the vis-NIR spectra and time scans. IR spectra were recorded with a Perkin Elmer 1650 Fourier transform infrared (FTIR) spectrophotometer. Cyclic voltammetry was performed for the SWNT/nafion/SWNT membrane without an electrolyte solution using a Bioanalytical System CV-27 potentiostat. A Ag/AgCl reference electrode was in contact with the SWNT surface via a small drop of 1M aqueous sulfuric acid serving as a “salt bridge” between the reference electrode and working electrode, which was on the same side of the membrane. The other side of the membrane was the counter electrode. Such a configuration allowed the study of the electrochemical reactions occurring in the interface area between the nanotubes and the nafion.

III. RESULTS AND DISCUSSION

A. FTIR, vis-NIR spectroscopy and cyclic voltammetry

FTIR and vis/NIR spectroscopy were employed to elucidate information such as structural or conformational changes that may occur during the actuation mechanism.

The FTIR spectrum of pure nafion (Fig. 2) shows two narrow bands (980 cm^{-1} and 1063 cm^{-1}), which can be assigned to C-F bonds of the nafion backbone and the side chains. An intense, broadband at 1200 cm^{-1} (off scale in Fig. 2) is assigned to an antisymmetric stretch of the sulfonate groups.¹¹ A strong broadband centered at 3470 cm^{-1} is attributed to fundamental hydrogen-bonded -OH stretching. After SWNT spraying onto nafion, the structure of the spectrum in the range of 4000–1000 cm^{-1} remained unchanged, although with a slight increase in scattering. The FTIR spectra were taken under various bias voltages up to 6 V, and retained the original characteristics with the exception of intensity changes in the pronounced peak at 3470 cm^{-1} . Figure 2 demonstrates the gradual decrease of this peak (3470 cm^{-1}) intensity (up to 12%) under increasing bias from 0 to 6 V. The intensity of this peak recovers to the initial value after the bias is returned to 0 V. The dynamic characteristics of the peak intensity with respect to applied voltage was recorded by a time scan at constant wave number (3470 cm^{-1}) synchronized with the voltage sweep (0–10 V) with a

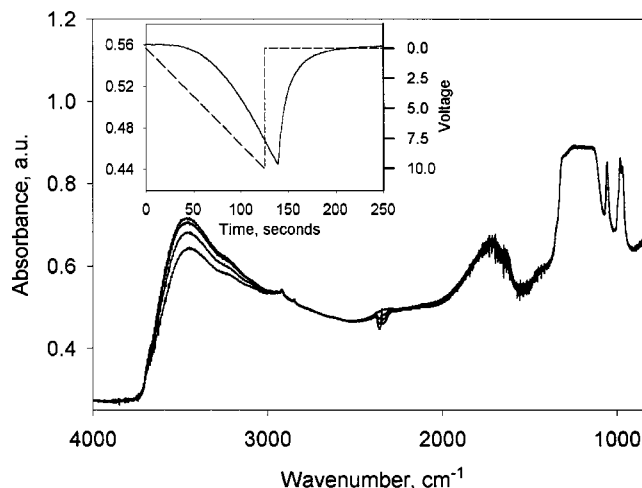


FIG. 2. FTIR spectra of SWNT/nafion/SWNT sample under electrical stimulation. (Inset) NIR time scan of absorbance peak (3470 cm^{-1}) during a voltage sweep.

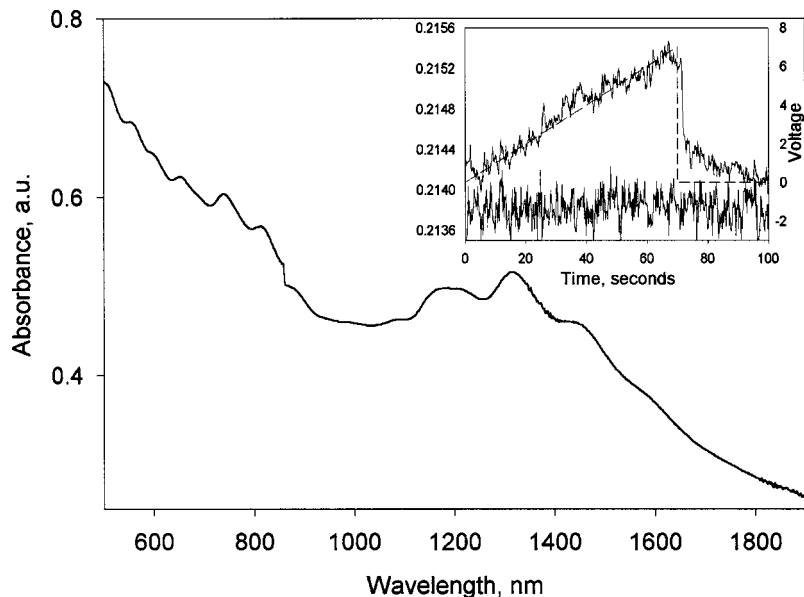
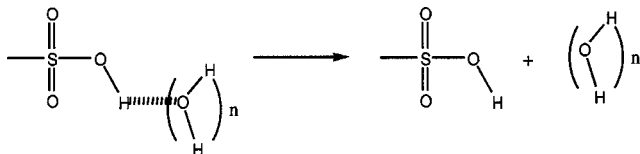


FIG. 3. Vis/NIR spectrum of SWNT/nafion/SWNT sample. The kink at 850 nm is a result of the lamp switch. (Inset) NIR time scan (1335 nm) of SWNT/nafion/SWNT during a voltage sweep.

rate of 0.2 V/s (Fig. 2, inset). When a bias of 10 V was applied a 20% decrease in peak intensity was observed but this was completely recovered after the bias was removed (Fig. 2, inset). These data ruled out the possibility of hydrolysis, since this would cause an irreversible change in the peak intensity. Intensity reversibility can be explained in terms of decreasing numbers of $-OH$ bonds, in accord with the hydrogen-bonding scheme shown below.



It is known that the sulfonate groups of the nafion side chains are capable of forming weak hydrogen bonds with the mobile protons and the water within the nafion.¹¹ Applied bias induces cation and electro-osmotic water transport^{2,6-8} resulting in the reduction of the number of $-OH$ bonds compared with their equilibrium concentration. The same mechanisms contribute to IPCM cantilever displacement, therefore the $-OH$ band intensity decrease can be attributed to the beginning of the actuation process. Also, in our case, as will be shown in the following section, SWNT/nafion/SWNT cantilever displacement starts at about 2 V, which is consistent with the sizable change in the $-OH$ peak intensity.

The vis-NIR absorption spectra of the SWNT/nafion/SWNT composite exhibited bands that are typical for semiconducting nanotubes (nafion is transparent in this spectral range). The broadband in the range of 1000–1700 nm corresponds to the first principal transition ($v_s^1 \rightarrow c_s^1$) between Van Hove singularities of the density of states of semiconducting SWNTs (Fig. 3).^{12,13} The fine structure of the band (1000–1700 nm) was similar to that observed for SWNTs prepared by the HiPco process¹³ and there are at least four subbands, which can be assigned to the distribution of nanotubes with different diameters in the range of 0.8–1.1 nm. As a reference, a SWNT/glass/SWNT sandwich was used (prepared under the same conditions for SWNT spraying as for the

SWNT/nafion/SWNT sample). It was found that for the SWNT/nafion/SWNT composite the absorbance intensity consistently increases with an increase of the applied voltage, distinct from the reference sample, which exhibited no voltage dependence. The same synchronized scan as used for the FTIR measurement was applied to detect the intensity change at constant wavelength for SWNT/nafion/SWNT and reference samples (Fig. 3, inset). An absorbance increase cannot be associated with the mechanical/position change of the SWNT/nafion/SWNT membrane as a result of actuation because, for optical measurements, the membrane was fixed from two sides in the holder. The absence of displacement in this configuration was confirmed by the Fresnel technique up to 10 V bias. This significant correlation between bias voltage and absorbance may be a result of complex changes in the dielectric constant (imaginary and real parts) of the interface medium between the SWNT and nafion due to the double-layer effect strongly affecting the local polarizability. Also, a transition of hydrated water to free water (as shown above) as a result of proton flux can contribute to the dielectric constant change, as will be discussed in the following section.

Cyclic voltammetry provides information regarding electrochemical reactions occurring at the interface between the SWNT and nafion. The peak at 0.5 V can be assigned to the oxidation of the oxygen-containing functional groups located on the SWNTs surface (Fig. 4). As reported in previous studies,^{13,14} the formation of surface oxides on SWNTs can be represented by an expression $=C=O + H^+ + e^- \rightleftharpoons =COH$. The weaker peak at ~ 1 V is likely due to a similar oxidation at different sites on the nanotubes (e.g., tube ends) or nanotubes of different chirality, analogous to the chemoselectivity recently demonstrated by Strano *et al.*¹⁵ The peak current at 0.5 V was found to have a nearly linear dependence on scan rate. This result indicates that the oxidation process occurs at the surface, according to the above expression, and excludes a diffusion process.

A correlation between the spectroscopic data and the cy-

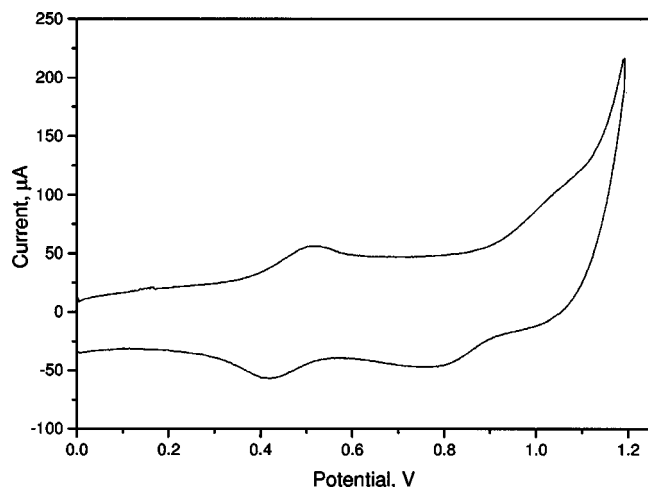


FIG. 4. Cyclic voltammogram of the SWNT/nafion/SWNT membrane.

cyclic voltammetry data can be explained by the exchange of mobile protons between the SWNTs and the nafion. The current induces a charge separation within the nafion, breaks hydrogen bonds, and results in the production of mobile protons. The protons on the cathode can, in turn, be used to reduce the surface oxides on the SWNT side of the interface. Also, we can conclude that the SWNT-nafion interface cannot be represented as a double-layer supercapacitor, in contrast to the results reported for SWNTs in aqueous NaCl solution.^{9(a),9(b)} In our case, the peak at 0.5 V indicates that an electrochemical process occurs at the SWNT-nafion interfacial area, which can affect the interface resistance and capacitance.

B. Electromechanical study

The mechanical response of the SWNT/nafion/SWNT bimorph cantilever under dc step voltage is shown in Fig. 5. The mechanism of actuation presumably can be associated with the electromechanical properties of both the SWNTs and the nafion, as mentioned before. To clarify the SWNT role in the composite's actuation two reference samples,

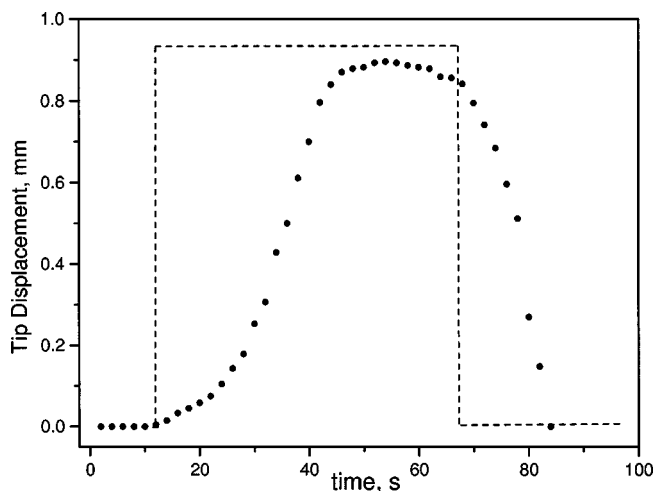


FIG. 5. Displacement of SWNT/nafion/SWNT cantilever driven by 3.5 V rectangular dc voltage.

sputtered gold/nafion/gold and sprayed graphite/nafion/graphite, were tested under the same conditions. Another set of reference samples, SWNT/*X*/SWNT where *X* is glass, paper, polyethylene (a nonionomeric polymer), and nanoporous alumina oxide soaked in the NaCl (1M) solution, was used to elucidate nafion's contribution to the mechanical response. All of these samples exhibited no actuation under applied dc bias in the range of 1–5 V. Thus, we can conclude that actuation occurs only for nafion-SWNT composites with a high interface area resulting in efficient current flow. A high ionic current through the composite due to proton mobility should induce swelling of the cathode side and consequently cantilever bending toward the anode side. Apparently, only SWNTs with a huge surface to volume ratio,^{9,12} with respect to other tested materials, can provide the current values necessary for the cantilever bending. Similar situations occurred for IPMC composites, where a high interface area is the result of the fractal-like microstructure between nafion and electrochemically plated platinum.² However, for the SWNT-nafion cross section, no interfacial fractal structure is observed on the micron scale (Fig. 1). This is likely to be associated with the nanoscale structure of nanotube bundles whose diameter of 50–100 nm defines the characteristic contact size between SWNTs and the polymer. Another distinction from IPMCs should be the contribution of SWNTs own actuation^{9(a),9(b)} (quantum effect), which amplifies the nafion displacement at low bias. However these two mechanisms are difficult to separate from each other. As can be seen in Fig. 5, the SWNT/nafion/SWNT actuator exhibits a minimum reversal displacement under applied step voltage, which is different from the IPMC actuators (Pt-nafion, and metal-ion exchanged form of nafion) in aqueous solutions.^{16,17} For example, the reverse displacement after 50 s was more than 50% for a Li⁺-nafion cantilever,¹⁷ and 100% after several seconds for Li⁺-, Na⁺-, Cs⁺-nafion and protonated nafion.¹⁶ The reversal mechanism in such cases can be associated with interfacial tension and water back diffusion due to osmotic pressures.^{6,16} Applied bias to protonated nafion in the SWNT/nafion/SWNT actuator induced mostly proton flow toward the cathode without strong involvement of the water molecules. Therefore, the back relaxation can be considerable lower than that for metal-ion-nafion forms. Also, because experiments were carried out in open air, the water concentration inside the nafion was less than that in the IPMC samples immersed in the water.^{6,16,17} In addition, the interfacial tension during actuation between SWNT and nafion can be less than tension between nafion and platinum due to a high SWNT elasticity.¹²

I-*V* characteristics for SWNT/nafion/SWNT, graphite/nafion/graphite, and gold/nafion/gold are consistent with our assumption about the high current flow through the SWNT-nafion interface. As can be seen from Fig. 6, beginning at 2.5 V the current density of the SWNT/nafion/SWNT sample is significantly higher than that of the reference samples. At the same voltage, the SWNT/nafion/SWNT cantilever begins to exhibit an actuation.

More detailed information about the actuation mechanisms can be obtained from the temporal current response to a step voltage. Figure 7 shows the current decay of SWNT/

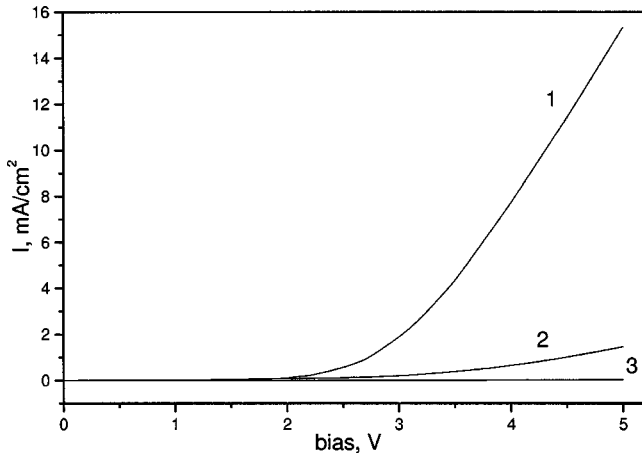


FIG. 6. I - V characteristics for SWNT/nafion/SWNT (1), graphite/nafion/graphite (2), and gold/nafion/gold (3) composites.

nafion/SWNT, graphite/nafion/graphite, and gold/nafion/gold samples as a response to a 3.5 V step voltage. The qualitative evaluation demonstrates at least two distinctive features between SWNT/nafion/SWNT and the reference samples. First, the SWNT/nafion/SWNT average lifetime is longer than that of graphite/nafion/graphite and gold/nafion/gold samples. Second, the SWNT/nafion/SWNT decay cannot be fitted by a monoexponential function while such a fit is quite satisfactory for the reference samples (Fig. 7). A biexponential function gives excellent fits to all experimental curves, but a pronounced difference between the monoexponential and biexponential fit is observed only for SWNT/nafion/SWNT composite. According to a previous study,¹⁷ a $\sim t^{-0.5}$ function should be more appropriate for the current response than an exponential decay if a fractal-like interface is responsible for actuation (distributed model). We did not find any satisfactory fit by the power function $\sim t^{-n}$ (even with a varied power n) to the experimental SWNT/nafion/SWNT decay, which is consistent with our SEM image of the interface (Fig. 1), where no fractal-like structure was observed. Hence,

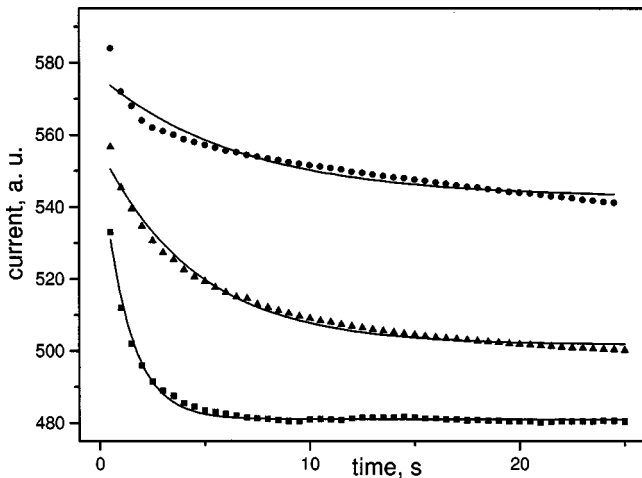


FIG. 7. Current time scans of SWNT/nafion/SWNT (circles), graphite/nafion/graphite (triangles), and gold/nafion/gold (squares) composites at applied step voltage of 3.5 V and monoexponential fit curves (solid lines).

biexponential decay with a long time component can be considered as a sign of an electromechanical effect [Fig. 8(a)].

To explain the above features we propose a model based on an electrical circuit that simulates the current-time response in the actuating system (Fig. 9). Here r_0 is the internal polymer resistance between SWNT electrodes; r_1 , c_1 , and r_2 , c_2 are leakage resistances and capacitances of both of the SWNT-nafion interfaces. The actuating process leads to an asymmetry in electrochemical properties of the cathodic and anodic interfaces, and consequently to the differences between resistances and capacitances at both sides of the cantilever. The solution of the current-time response, $i(t)$ on the step voltage ϵ , for such a circuit is as follows:

$$i(t) = B_1 \exp(-z_1 t) + B_2 \exp(-z_2 t) + B_0, \quad (1)$$

where $z_1 = \delta_1 + \delta_2$, $z_2 = \delta_1 - \delta_2$,

$$\delta_1 = \frac{c_1 \left(1 + \frac{r_0}{r_2}\right) + c_2 \left(1 + \frac{r_0}{r_1}\right)}{2c_1 c_2 r_0},$$

$$\delta_2 = \frac{\left(\left[c_1 \left(1 + \frac{r_0}{r_2}\right) - c_2 \left(1 + \frac{r_0}{r_1}\right)\right]^2 + 4c_1 c_2\right)^{1/2}}{2c_1 c_2 r_0}, \quad (2)$$

$$\chi = \frac{\epsilon}{(z_2 - z_1)(r_0 + r_1 + r_2)r_0 r_1 c_1}, \quad (3)$$

$$B_1 = \chi(r_0 + r_1 + r_2 - z_2 r_0 r_1 c_1)(1 - r_1 c_1 z_1),$$

$$B_2 = -\chi(r_0 + r_1 + r_2 - z_1 r_0 r_1 c_1)(1 - r_1 c_1 z_2), \quad (4)$$

$$B_0 = \frac{\epsilon}{r_0 + r_1 + r_2}. \quad (5)$$

The current decay of the SWNT/nafion/SWNT sample at step voltages below and above the actuating threshold (Fig. 8) exhibits a significant difference in the $i(t)$ function (Table I). At low voltage (0.8 V) the decay is almost monoexponential ($B_1/B_2 \sim 10, B_1/B_0 \sim 40$) and the major contribution is defined by the short-time component (0.5 s). At voltages of 3.5 V and greater (i.e., above the actuation threshold) the contribution of the long-time component is increased dramatically along with an increase of the background value ($B_1/B_2 \sim 1, B_1/B_0 < 0.1$). Also, the magnitude of $\tau_2 = z_2^{-1}$ is increased by a factor of 3 with respect to the low voltage case. The $i(t)$ decay can be described by a monoexponential function according to the above model (Fig. 9) if $r_1 = r_2 = r$ and $c_1 = c_2 = c$. Then,

$$i(t) = \frac{\epsilon}{r_0 + 2r} \left(1 + \frac{2r}{r_0}\right) \exp\left(-\frac{t}{Rc}\right),$$

where

$$R = \frac{r_0 r}{r_0 + 2r}. \quad (6)$$

This is consistent with the low voltage case when no actuation is observed and consequently there is no asymmetry in the properties of both sides of the cantilever (i.e., equal in-

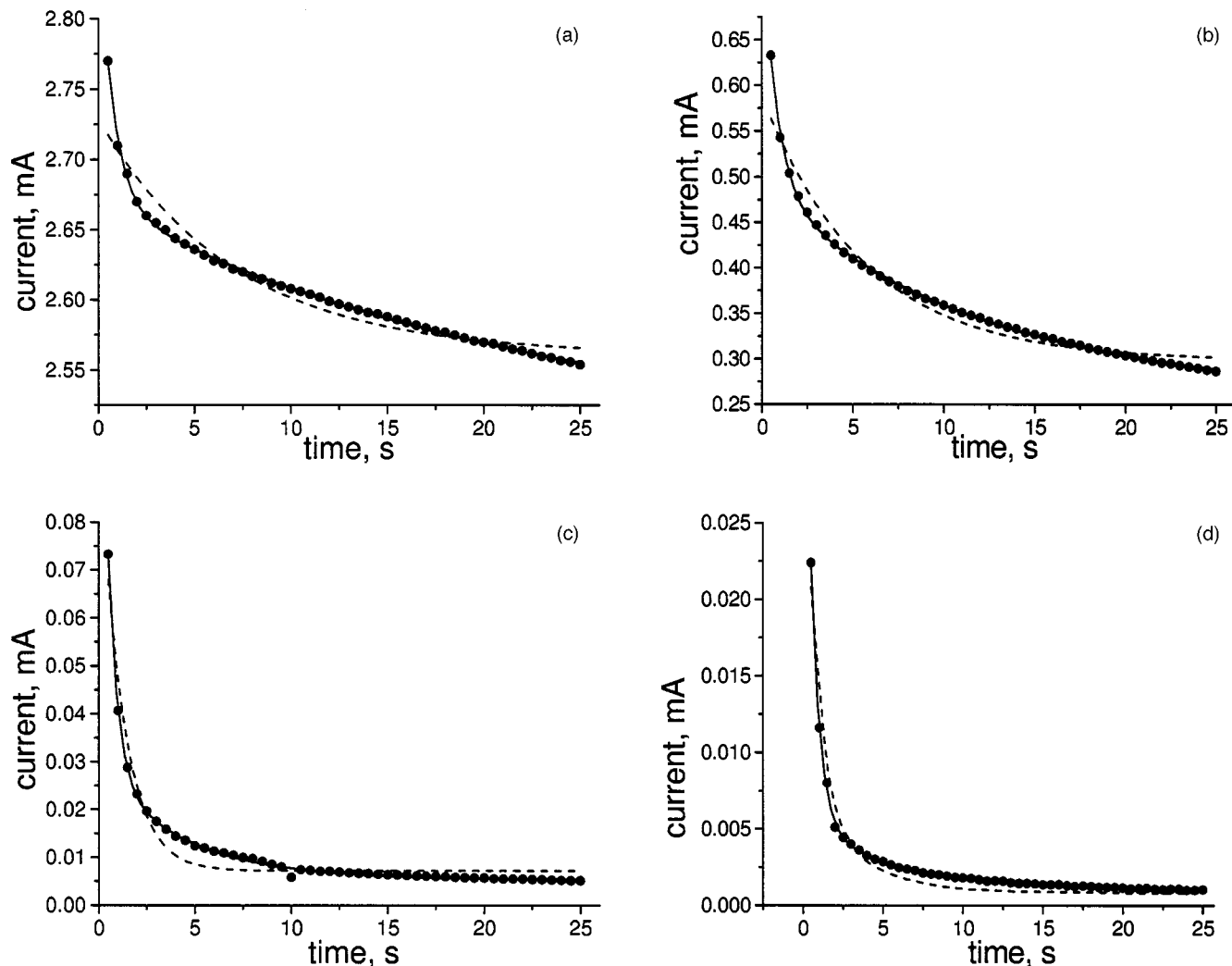


FIG. 8. Current time scans of SWNT/nafion/SWNT cantilever at applied step voltage of 3.5 V (a), 2.5 V (b), 1.5 V (c), and 0.8 V (d) and corresponding monoexponential (dash) and biexponential (solid) fit curves.

interface capacitances and resistors). The monoexponential fit of the experimental decay (0.8 V) by Eq. (6) gives $r_0 = 20 \text{ k}\Omega$, $r = 400 \text{ k}\Omega$, and $c = 60 \mu\text{F}$.

For the $i(t)$ dependence at 3.5 V (biexponential decay) we can make quantitative conclusions about the resistances and capacitances. Using the asymptotic behavior of Eq. (1) and simple approximations, c_1 , c_2 , r_0 , r_1 , and r_2 can be expressed via z_1 , z_2 , B_0 , B_1 , and B_2 . First, according to Eq. (5) and the B_0 fit value, the sum of the resistances is $r_0 + r_1 + r_2 = 1.4 \text{ k}\Omega$, which indicates considerable reduction

of the resistances compared with the low voltage case: at least one order of magnitude for the internal polymer resistance (r_0) and two orders for the leakage/interface resistances (r_1, r_2). Second, as the z_1 parameter is much higher than z_2 ($z_1 \gg z_2$, Table I), an approximation $\delta_1 = \delta_2$ is possible and from Eq. (2) it follows that $r_0^{-1} \approx r_1^{-1} + r_2^{-1} + r_0/(r_1 r_2)$ leading to $r_1, r_2 \gg r_0$. A similar relationship between interface and internal resistances for voltages below the actuation threshold was found. Hence, an actuation process reduces not only interface resistances but also the internal polymer resistance, and this value is lower than that at the SWNT-nafion interface. Third, from the above conditions ($\delta_1 \approx \delta_2$) it follows that $z_1 \approx 2 \delta_2 = c_1^{-1}(r_0^{-1} + r_1^{-1})$

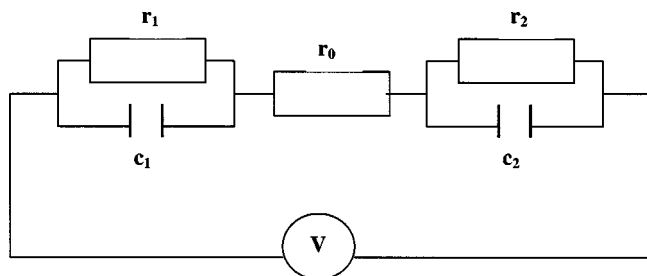


FIG. 9. Electrical circuit simulating the current response in the SWNT/nafion/SWNT composite.

TABLE I. Parameters for the best fit of the $i(t)$ function by biexponential decay at different values of the step voltage.

Volts	τ_1 (s)	z_1 (s^{-1})	τ_2 (s)	z_2 (s^{-1})	B_1/B_2	B_1/B_0
0.8	0.5	2.0	5.2	0.19	9.2	41
1.5	0.5	2.0	4.7	0.21	5.3	24
2.5	0.7	1.43	11.8	0.084	1.3	1.1
3.5	0.7	1.43	21.8	0.046	1.1	0.08

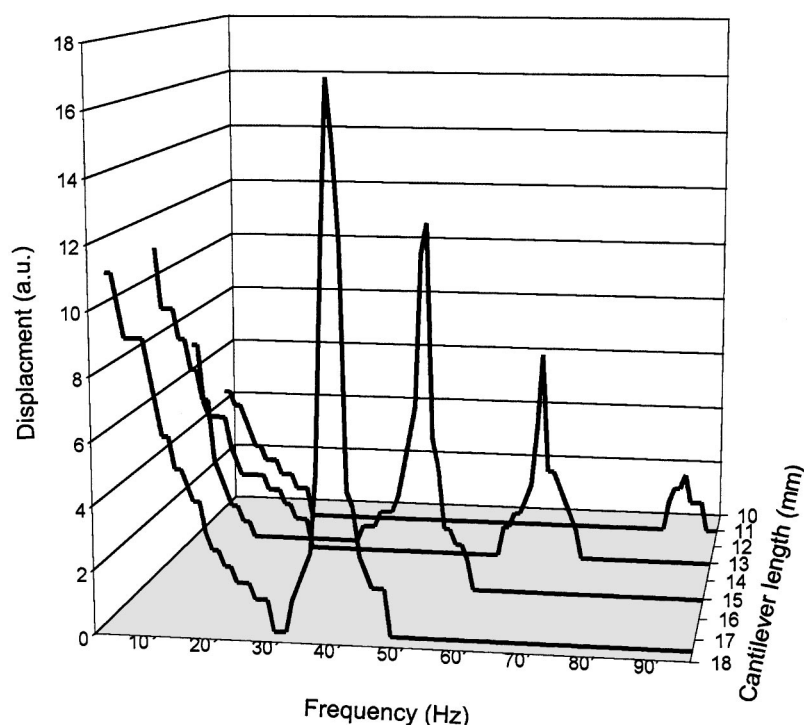


FIG. 10. SWNT/nafion/SWNT cantilever displacement at an ac bias of 3.5 V as a function of the frequency at different cantilever lengths.

$+c_2^{-1}(r_0^{-1}+r_2^{-1})$. As r_0 , r_1 , and $r_2 < 1.4 \text{ k}\Omega$, then r_0^{-1} , r_0^{-1} , and $r_2^{-1} > 7.1 \times 10^{-4} \Omega^{-1}$, which gives $z_1 \geq 1.4 \times 10^{-3} (c_1^{-1} + c_2^{-1})$. Taking $z_1 = 1.43 \text{ s}^{-1}$ (Table I), we can get an estimate for the interface capacitances under actuation: c_1 , $c_2 \geq 1 \text{ mF}$.

A decrease of the resistances and increase of the capacitances can be understood in terms of ionic conductivity, change of the water dielectric constant, and electrostatic expansion of the SWNTs with charge injection. When an applied bias is enough to induce proton flux from the anode to the cathode, internal and interfacial resistances are reduced due to imbalanced charge carriers. According to the model,^{7,8} such a redistribution of mobile cations results in polymer chain contraction between nafion hydrophilic clusters at the anodic side and chain expansion at the cathode. This electrostatic mechanism of cantilever bending should prevail over water osmotic stress by at least in one order of magnitude,⁷ especially for our case: nafion is not water swollen; open-air conditions (nonaqueous environment); and proton transport (as distinct from metal cation transport) does not necessarily involve the water molecules.⁸ However, even in the relatively dry nafion, there is enough hydrated water (bound to protons) to strongly affect the dielectric constant upon applied bias.

It is known that free water has a dielectric constant of 78 at room temperature and this value can be reduced by an order of six for hydrated water bound to ions in the solvents.¹⁸ When an electric field moves protons, an excess of free water near the anodic side can strongly increase the dielectric constant at the SWNT-nafion interface. Moreover, at the cathode side the protons bind to the surface oxides of SWNTs (as was discussed previously) and cannot participate in the water hydration, which results in an increase of the free water at the cathode interface and consequently an in-

crease of the dielectric constant. Since interface capacitance is given as $c \sim (\epsilon/d)S$, where ϵ is the dielectric constant, S is the SWNT-nafion contact surface, and d is the thickness of the interface double layer, the ϵ value change should increase the interface capacitance at both sides of SWNT/nafion/SWNT cantilever. Also, charge injection in the SWNTs should enlarge the SWNT-nafion contact surface S due to electrostatic repulsion between SWNT bundles and individual nanotubes inside the bundles.¹⁹ This effect can also contribute to increase of the interface capacitances.

Of special interest presents is the cantilever response to ac voltage and dependence of its displacement on ac frequency. We detected the cantilever displacement in the frequency range up to 100 Hz with ac voltage 2.5, 3.5, and 5 V (sine function). It was found that SWNT/nafion/SWNT samples have resonance frequencies depending on cantilever size. According to expectations, the resonance frequency peak was shifted to higher frequency with reduction of its length (Fig. 10). The SWNT-nafion composite demonstrates a high robustness with respect to the graphite-nafion reference sample. Carbon nanotube material sprayed onto the nafion surface was strongly adhered and did not show any aging or peeling for more than two months after composite preparation and storage at normal conditions. In contrast, the graphite adhesion was poor and the graphite layer could be easily removed from the nafion surface. Cantilevers fabricated from the fresh SWNT-nafion composite and from an aged composite (two months) did not exhibit any difference in actuation properties. Also, we tested the actuation lifetime under ac signal at the resonance frequency: the cantilever demonstrated remarkable continuous actuation for 810 000 cycles (6.25 h, 36 Hz, 1.2 V) at the resonance frequency with an amplitude reduction of less than 10% from the initial value.

In conclusion, we have shown that trilayer composites of nafion and single-walled carbon nanotubes can be used to fabricate effective actuating systems. The actuators give sizable response under modest voltages and in the absence of a supporting electrolyte. The mechanism of actuation is similar to the traditional IPMC systems at high applied voltages, depending upon an electrostatic imbalance at the two sides of the cantilever. This conclusion was supported by an electrical circuit model that allowed us to estimate the changes in the interfacial resistances and capacitances in the actuator. The parameters determined using this model imply a significant change in the proton flux in the nafion under applied bias, which was consistent with the decrease of the hydrogen bonding stretch in the FTIR spectrum. The vis-NIR spectroscopy suggested that the semiconducting SWNTs were responsible for some of the actuation, implying that there is a contribution from quantum effects in the SWNTs, as well. Finally, the large surface area of the SWNTs appears to be an important component in these systems.

ACKNOWLEDGMENTS

This work was supported by the Missile Defense Agency Grant No. F29601-02-C-0270. The authors are grateful to Dr. M. Cheng for her help in the CV measurements and M. Platek for his help in optical and SEM imaging.

¹Y. Bar-Cohen, *Electroactive Polymer Actuators as Artificial Muscles* (SPIE, Bellingham, WA, 2001).

²(a) Shahinpoor, Y. Bar-Cohen, J. O. Simpson, and J. Smith, *Smart Mater. Struct.* **7**, R15 (1998); (b) K. Sadeghipour, R. Salomon, and S. Neogi, *ibid.* **1**, 172 (1992); (c) K. Onishi, S. Sewa, K. Asaka, N. Fujiwara, and K. Oguro, *Electrochim. Acta* **46**, 737 (2000).

³K. Tashiro and H. S. Nalwa, *Ferroelectric Polymers* (Dekker, New York, 1995), pp. 63–181.

⁴Y. Osada, H. Okuzaki, and H. Hori, *Nature (London)* **355**, 242 (1992); Z.

Liu and P. Calvert, *Adv. Mater. (Weinheim, Ger.)* **12**, 288 (2000).

⁵M. J. Marsella and R. J. Reid, *Macromolecules* **32**, 5982 (1999); T. F. Otero and J. M. Sansinena, *Adv. Mater. (Weinheim, Ger.)* **10**, 491 (1998); K. Kaneto, M. Kaeko, Y. Min, and A. G. MacDiarmid, *Synth. Met.* **71**, 2211 (1995).

⁶K. Asaka and K. Oguro, *J. Electroanal. Chem.* **480**, 186 (2000).

⁷S. Nemat-Nasser and J. Y. Li, *J. Appl. Phys.* **87**, 3321 (2000).

⁸S. Nemat-Nasser and C. W. Thomas, *Electroactive Polymer Actuators as Artificial Muscles*, edited by Y. Bar-Cohen (SPIE, Bellingham, WA, 2001), pp. 139–191.

⁹(a) R. H. Baughman, C. Cui, A. A. Zakhidov *et al.*, *Science* **284**, 1340 (1999); (b) G. M. Spinks, G. G. Wallace, R. H. Baughman, and L. Dai, *Electroactive Polymer Actuators as Artificial Muscles*, edited by Y. Bar-Cohen (SPIE, Bellingham, WA, 2001), pp. 223–246; (c) G. M. Spinks, G. G. Wallace, L. S. Fifield, R. L. Dalton, A. Mazzoldi, D. De Rossi, I. I. Khayrullin, and R. H. Baughman, *Adv. Mater. (Weinheim, Ger.)* **14**, 1728 (2002).

¹⁰D. Chattopadhyay, I. E. Galeska, F. Papadimitrakopoulos, E. Munoz, and R. H. Baughman, *Proc. SPIE* **52–56**, 4695 (2002); B. J. Landi, R. P. Raffaele, M. J. Heben, J. L. Alleman, W. VanDerveer, and T. Gennett, *Nano Lett.* **2**, 1329 (2002).

¹¹R. M. Blanchard and R. G. Nuzzo, *J. Polym. Sci., Part B: Polym. Phys.* **38**, 1512 (2000).

¹²*Carbon Nanotubes: Synthesis, Structure, Properties and Applications*, edited by M. Dresselhaus, G. Dresselhaus, and Ph. Avouris (Springer, Berlin, 2001).

¹³L. Kavan, P. Rapt, L. Dunsch, M. J. Bronikowski, P. Willis, and R. E. Smalley, *J. Phys. Chem. B* **105**, 10764 (2001).

¹⁴J. N. Barisci, G. G. Wallace, and R. H. Baughman, *J. Electrochem. Soc.* **147**, 4580 (2000).

¹⁵M. S. Strano, C. A. Dyke, M. L. Usrey, P. W. Barone, M. J. Allen, H. Shan, C. Kittrell, R. H. Hauge, J. M. Tour, and R. E. Smalley, *Science* **301**, 1519 (2003).

¹⁶Y. Abe, A. Mochizuki, T. Kawashima, S. Yamashita, K. Asaka, and K. Oguro, *Polym. Adv. Technol.* **9**, 520 (1998).

¹⁷X. Bao, Y. Bar-Cohen, and S.-S. Lih, in *Proceedings of the SPIE, Smart Structure and Materials Symposium*, San Diego, CA, 18–21 March, 2002, paper 4695-27.

¹⁸O'M. J. Bokris and A. K. N. Reddy, *Modern Electrochemistry* (Plenum, New York, 1998), Vol. 1.

¹⁹Y. Zang and S. Iijima, *Phys. Rev. Lett.* **17**, 3472 (1999).